

A Defect Supertetrahedron Naphthoxime-Based $[\text{Mn}^{\text{III}}_9]$ Single-Molecule Magnet

Małgorzata Hołyńska,^{*,†} Nicolas Frank,[†] Céline Pichon,^{‡,§} Je-Rang Jeon,^{‡,§} Rodolphe Clérac,^{*,‡,§} and Stefanie Dehnen[†]

[†]Fachbereich Chemie and Wissenschaftliches Zentrum für Materialwissenschaften (WZMW), Philipps-Universität Marburg, Hans-Meerwein-Straße, D-35032 Marburg, Germany

[‡]CNRS, CRPP, UPR 8641, F-33600 Pessac, France

[§]Univ. Bordeaux, CRPP, UPR 8641, F-33600 Pessac, France

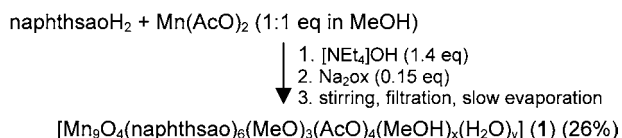
Supporting Information

ABSTRACT: A new $[\text{Mn}^{\text{III}}_9]$ complex was synthesized from a naphthoxime-based ligand. It was structurally and magnetically characterized, revealing a rare defect supertetrahedral topology and promising SMM properties with a large energy barrier of 67 K.

The search for new molecular topologies is an important part of the *Single Molecule Magnet* (SMM) design.¹ A variety of novel molecular architectures has been reported for polynuclear manganese complexes with a growth of their complexity going in concert with the increase of their nuclearity. Many polynuclear complexes, which possess interesting magnetic properties, involve manganese ions; the largest aggregate reported to date is the $[\text{Mn}_{84}]$ complex described by Christou et al.² with acetate acting as ligands. In the chemistry of oxime-bridged Mn complexes,³ the highest-nuclearity ones are the double-decker $[\text{Mn}_{32}]$ wheel^{4a} and an unusual 2-pyridylaldoximate-based $[\text{Mn}^{\text{II/III}}_{15}]$ complex with an $S_T = 6$ ground state.^{4b} The use of this oxime ligand along with azide co-ligands also allowed the synthesis of unique high-nuclearity $[\text{Ni}_{14}]$ and $[\text{Ni}_{12}\text{Na}_2]$ complexes.⁵

Following our strategy to synthesize oxime-based polynuclear SMMs with magnetically anisotropic Mn^{III} metal ions, we used a new naphthoxime-based ligand (1-(1-hydroxynaphthalen-2-yl)-ethanone oxime, naphthsaoH₂).⁶ A series of $[\text{Mn}_3]$ complexes with carboxylates as terminal co-ligands was synthesized and characterized.⁶ To explore the effect of additional carboxylate moieties, we performed a reaction involving manganese(II) acetate with naphthsaoH₂ in a basic methanol solution in the presence of sodium oxalate (Scheme 1). This led to single crystals of the $[\text{Mn}^{\text{III}}_9]$ complex **1** with a

Scheme 1. Synthesis Steps for the Formation of **1 (ox = oxalate; x:y = 1:1 or 2:0; See Supporting Information for More Details)**



defect supertetrahedral topology (preceded by an $[\text{Mn}_3]$ complex—see Supporting Information). Investigations of the magnetic properties indicate that **1** exhibits SMM behavior with a relatively large energy barrier of 67 K.

The obtained crystals have a tendency to form polysynthetically twinned aggregates, which seems to be intrinsic to this compound (see Supporting Information). Attempts to overcome this by changing solvents or reaction conditions were unsuccessful. The rare-topology complex **1** was formed in a reaction in alcoholic solution normally producing $[\text{Mn}_3]$ or $[\text{Mn}_6]$ products.³ In the presence of sodium oxalate, **1** is the sole product, which cannot be explained so far. Compound **1** crystallizes in the monoclinic space group $C2/c$, with an $[\text{Mn}_9]$ skeleton close to C_3 symmetry that was previously reported by Wang et al. and Inglis et al.⁷ In this skeleton, the nine Mn^{III} ions occupy the vertices of a defect supertetrahedron missing one vertex (Figure 1).

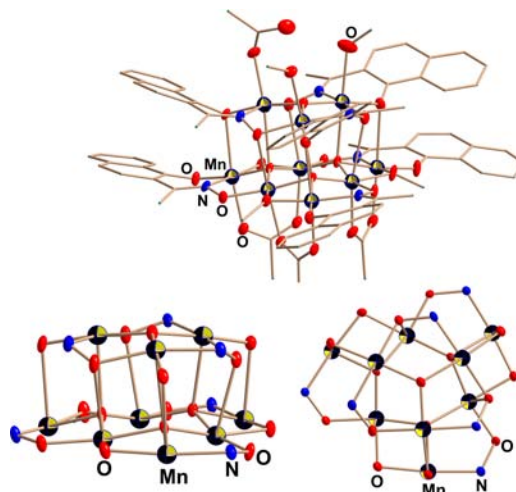


Figure 1. Different views of the $[\text{Mn}_9]$ complex in **1** (top, ellipsoids of Mn, N, O atoms at 20% probability level, C atoms as wires, H atoms omitted for clarity) and zoom of the C_3 symmetric complex core omitting the organic groups (bottom, side and top views).

Received: April 24, 2013

Published: June 13, 2013

The defect-supertetrahedral $[\text{Mn}_9]$ complex is composed of two main units. The first one contains three Mn^{III} ions linked by a central μ_3 -oxido ligand. The sides of this $[\text{Mn}_3]$ triangle are bridged by oxime groups from three naphthsao ligands. The second unit comprises six Mn^{III} atoms, which form the vertices and the edge centers of a larger triangle. Three oxido ligands are situated inside this $[\text{Mn}_6]$ moiety, linking the vertex sites with the two adjacent edge-centering Mn^{III} ions. Three naphthsao oxime groups and three μ -methoxido/*syn-syn* acetato ligands alternately bridge the neighboring Mn^{III} centers around the $[\text{Mn}_6]$ triangular motif. The $[\text{Mn}_3]$ and $[\text{Mn}_6]$ units are connected to form the $[\text{Mn}_9]$ skeleton in **1** (Figure 1, Scheme S1), being linked through three different types of O donor atoms: (1) three phenoxido or (2) three oxime O atoms from the $[\text{Mn}_3]$ naphthsao ligands bridging the three Mn^{III} atoms of the $[\text{Mn}_3]$ unit to the vertices and to the edge-centering Mn^{III} ions of the triangular $[\text{Mn}_6]$ moiety, respectively, or (3) three oxido ligands (now μ_4 -bridging) within the $[\text{Mn}_6]$ unit, which coordinate to the three Mn^{III} centers of the $[\text{Mn}_3]$ unit.

The terminal ligands of the $[\text{Mn}_3]$ unit are a monodentate acetate ligand beside methanol/water ligands (see Supporting Information). The naphthyl rings from the $[\text{Mn}_3]$ and $[\text{Mn}_6]$ naphthsao ligands are not involved in significant intramolecular stacking interactions, with the exception of two very weak contacts with an average intercentroid distance of about 3.6 Å (see Supporting Information). **1** is not stabilized by any other significant hydrogen bonds or stacking interactions. The complexes form columns extending along *b* (Figure S1). As the X-ray diffraction data for **1** are always affected by twinning, the geometric parameters will not be discussed in more detail. However, the +3 oxidation state of the Mn ions is consistent with the presence of a Jahn–Teller distortion, and the shortest intracomplex Mn⋯Mn distances are 2.707(2)–3.534(2) Å.

The isomorphous prototype $[\text{Mn}_9]$ complexes reported by Wang et al., $[\text{Mn}_9\text{O}_4(\text{Mesao})_6(\text{MeO})_3(\text{O}_2\text{CMe})_3(\text{OH})(\text{MeOH})_2] \cdot 2.5\text{DMF}$ (**A**),^{7a} and Inglis et al., $[\text{Mn}_9\text{O}_4(\text{OMe})_4(\text{OAc})_3(\text{Mesao})_6(\text{H}_2\text{O})_2] \cdot 1.5\text{H}_2\text{O}$ (**B**),^{7b} were obtained in reactions of manganese(II) acetate and Me-saoH₂ (2-hydroxyphenylethanone oxime) in $\text{CH}_3\text{OH}/\text{DMF}$, followed by layering with diethyl ether (**A**) or by the addition of different salts, e.g. lanthanum(III) nitrate, to a solution of manganese(II) acetate, Me-saoH₂, and triethylamine in methanol (**B**). The molecular structures of these two compounds are very similar to **1** (one of the differences concerns the relative oxime groups arrangement—see Figure S1b, Supporting Information). A CCDC database search⁸ provides examples of 17 nonanuclear Mn^{III} complexes.^{7,9–19}

As both **A** and **B** complexes display SMM properties, the magnetic properties of **1** have been investigated. The temperature dependence of the χT product at 1000 Oe is shown in Figure 2. At room temperature, the χT product is 20.3 $\text{cm}^3 \text{K/mol}$ and is significantly lower than the expected value (27 $\text{cm}^3 \text{K/mol}$) for nine non-interacting Mn^{III} $S = 2$ spin carriers ($S = 2$, $C = 3 \text{ cm}^3 \text{K/mol}$ with $g = 2$). When the temperature is lowered, the χT product decreases, reaching 15.7 $\text{cm}^3 \text{K/mol}$ at 60 K, revealing the presence of dominant antiferromagnetic interactions within the $[\text{Mn}^{\text{III}}_9]$ complex and explaining the low value of the χT product at room temperature. Below 60 K, the χT product increases up to 17.5 $\text{cm}^3 \text{K/mol}$ at 12 K as expected when competing magnetic interactions lead to a ferrimagnetic arrangement of the spins within a complex. At lower temperatures, the χT product decreases as an indication of weak intercomplex antiferromag-

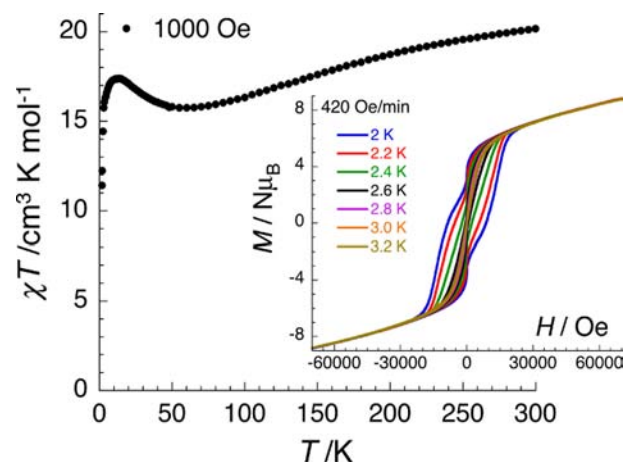


Figure 2. Temperature dependence of the χT product at 1000 Oe for **1** (with χ defined as molar magnetic susceptibility equal to M/H per mole of **1**). Inset: M vs H data at 420 Oe/min below 3.2 K for **1**, illustrating the slow relaxation of the magnetization, i.e., the presence of a hysteresis effect.

netic interactions and/or most likely due to the magnetic anisotropy (expected for Mn^{III} metal ions) as indeed confirmed by the linear increase of the 2 K magnetization at high fields and the nonsuperposition of the M vs H/T data (Figures 2 inset and S2). Due to the large number of magnetic centers and the complicated topology of the magnetic interactions in **1**, modeling of the magnetic susceptibility and thus fitting of the experimental data were not possible. Nevertheless, the combined χT vs T and M vs H data ($M_{(1.8\text{K}/7\text{T})} = 8.8 \mu_B$; Figures 2 and S2) suggest an $S_T = 6$ ground state, i.e., $\chi T_{(12\text{K})} = 17.5 \text{ cm}^3 \text{K/mol}$ being too high for $S_T = 5$ and too low for an $S_T = 7$ ground state.

Below 3 K, hysteresis effects are observed on the M vs H data, highlighting the magnet-type behavior of the complex, i.e. slow relaxation of the magnetization (Figures 2, inset, and S3). At 2 K, with a field-scanning rate of about 420 Oe/min, the coercive field reaches 0.87 T. It is worth noting that thermal avalanches are systematically observed below 2 K, and it is thus difficult to estimate the coercive field at lower temperatures.

The slow relaxation of the magnetization and its associated relaxation time has been studied by ac susceptibility measurements, which were performed below 15 K for ac frequencies up to 1.5 kHz. The data shown in Figure 3 reveal a non-zero out-of-phase response expected in the presence of slow relaxation of the magnetization. The *Single Molecule Magnet* (SMM) properties of **1** are clearly confirmed by the specific frequency and temperature dependences of both ac susceptibility components. The blocking temperature estimated at 1.5 kHz is 5.7 K. Using the whole set of ac data (Figure 3), the temperature dependence of the relaxation time, τ , shown in the inset of Figure 3 as a τ vs $1/T$ plot, has been determined.

The relaxation time is thermally activated with an energy barrier (Δ) of 67 K (between 3.5 and 6.2 K) and a pre-exponential factor of about 1.1×10^{-9} s. The SMM energy barrier of 67 K found in **1** is the highest reported for this family of $[\text{Mn}^{\text{III}}_9]$ complexes.⁷ It is almost twice as large as that for **A** (35.2 K) and **B** (30 K), while the spin ground state of the $[\text{Mn}^{\text{III}}_9]$ complexes appears to be the same ($S_T = 6$). Considering the $S_T = 6$ ground state of **1** and $\Delta/k_B = DS_T^2/k_B = 67 \text{ K}$, the D parameter²⁰ can be estimated at about -1.9 K ,

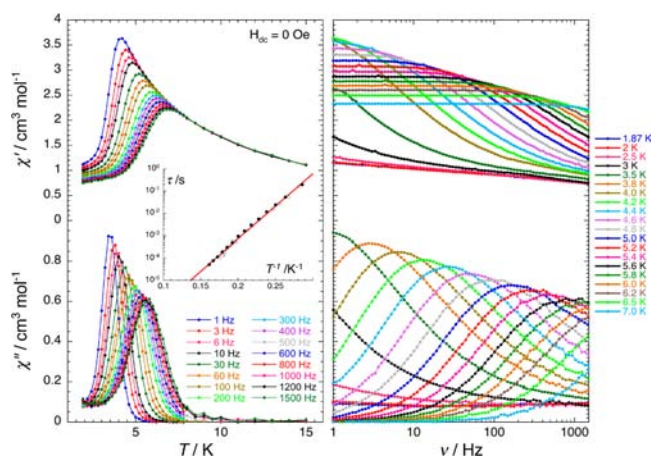


Figure 3. Temperature dependence below 15 K (left) and frequency dependence between 1 and 1500 Hz (right) of the in-phase (χ' , top) and out-of-phase (χ'' , bottom) components of the ac susceptibility at different frequencies (left) and temperatures (right) with a 3 Oe ac field in a zero dc field. Solid lines are guides for the eye. Inset: τ vs T^{-1} plot in zero dc field. The red solid line represents the best fit to the Arrhenius law between 3.5 and 6.2 K from the frequency (full dots) and temperature (open dots) dependences of the ac susceptibility.

which is much larger than the reported values for **A** (−1.1 K) and **B** (−0.9 K).

In conclusion, a new $[\text{Mn}^{\text{III}}_9]$ naphthoxime-based SMM was synthesized and fully characterized. Slow relaxation of the magnetization is observed at higher temperatures than for related complexes, due to a particularly strong uniaxial magnetic anisotropy ($D/k_B = -1.9$ K) and thus the large associated energy barrier ($\Delta/k_B = 67$ K).⁷ These characteristics are the result of the choice of a naphthoxime-based ligand with large peripheral aromatic rings. This ligand modifies the geometry of the $[\text{Mn}_9]$ skeleton with a better alignment of the Jahn–Teller Mn^{III} axes (corresponding to the local magnetic easy axes). Thus, the angle from a virtual central axis of symmetry is of 12.0–18.0° in **1**, whereas different values are observed in **A** (5.9, 8.1, 17.2°) and **B** (5.8, 8.7, 17.4°) different values are observed (see also comparison of Mn–N–O–Mn torsion angles in Supporting Information, Table S2). Similar synthetic approaches to increase the magnetic anisotropy of known SMMs are currently developed in our laboratories.

■ ASSOCIATED CONTENT

📄 Supporting Information

CIF of **1**, details of syntheses, IR spectra, details of magnetic properties measurements, X-ray data collection, structure refinement. This material is available free of charge via the Internet at <http://pubs.acs.org>.

■ AUTHOR INFORMATION

Corresponding Author

*E-mail: mholynska@gmail.com, clerac@crpp-bordeaux.cnrs.fr.

Author Contributions

M.H. and N.F. performed syntheses and structural analyses; R.C., C.P., and I-R.J. collected X-ray diffraction data, performed magnetic measurements, and detailed analysis. All authors cowrote the paper.

Funding Sources

Alexander von Humboldt Foundation, German Science Foundation (DFG), ANR (NT09_469563, AC-MAGnets project), and CNRS.

Notes

The authors declare no competing financial interest.

■ ACKNOWLEDGMENTS

We thank the Université Bordeaux, the ANR, the Region Aquitaine, the GIS Advanced Materials in Aquitaine (COMET Project), the CNRS, Alexander von Humboldt, and the German Science Foundation (DFG) for financial support.

■ REFERENCES

- (1) (a) Bagai, R.; Christou, G. *Chem. Soc. Rev.* **2009**, *38*, 1011. (b) Leuenberger, M. N.; Loss, D. *Nature* **2001**, *410*, 789. (c) Aromi, G.; Brechin, E. K. *Struct. Bonding (Berlin)* **2006**, *122*, 1. (d) Gatteschi, D.; Sessoli, R. *Angew. Chem., Int. Ed.* **2003**, *42*, 268. (e) Christou, G.; Gatteschi, D.; Hendrickson, D. N.; Sessoli, R. *MRS Bull.* **2000**, *25*, 66.
- (2) Tasiopoulos, A. T.; Vinslava, A.; Wernsdorfer, W.; Abboud, K. A.; Christou, G. *Angew. Chem., Int. Ed.* **2004**, *43*, 2117.
- (3) (a) Milios, C. J.; Vinslava, A.; Wernsdorfer, W.; Moggach, S.; Parsons, S.; Perlepes, S. P.; Christou, G.; Brechin, E. K. *J. Am. Chem. Soc.* **2007**, *129*, 2754. (b) Milios, C. J.; Inglis, R.; Vinslava, A.; Bagai, R.; Wernsdorfer, W.; Parsons, S.; Perlepes, S. P.; Christou, G.; Brechin, E. K. *J. Am. Chem. Soc.* **2007**, *129*, 12505. (c) Inglis, R.; Jones, L. F.; Milios, C. J.; Datta, S.; Collins, A.; Parsons, S.; Wernsdorfer, W.; Hill, S.; Perlepes, S. P.; Piligkos, S.; Brechin, E. K. *Dalton Trans.* **2009**, 3403.
- (4) (a) Manoli, M.; Inglis, R.; Manos, M. J.; Nastopoulos, V.; Wernsdorfer, W.; Brechin, E. K.; Tasiopoulos, A. J. *Angew. Chem., Int. Ed.* **2011**, *50*, 4441. (b) Alexandropoulos, D. I.; Papatriantafyllopoulou, C.; Aromi, G.; Roubeau, O.; Teat, S. J.; Perlepes, S. P.; Christou, G.; Stamatatos, T. C. *Inorg. Chem.* **2010**, *49*, 3962.
- (5) Stamatatos, T. C.; Abboud, K. A.; Perlepes, S. P.; Christou, G. *Dalton Trans.* **2007**, 3861.
- (6) Holyńska, M.; Frank, N.; Dehnen, S. *Z. Anorg. Allg. Chem.* **2012**, *638*, 2248.
- (7) (a) Wang, S.; Kong, L.; Yang, H.; He, Z.; Zheng, J.; Li, D.; Zeng, S.; Niu, M.; Song, Y.; Dou, J. *Inorg. Chem.* **2011**, *50*, 2705. (b) Inglis, R.; White, F.; Piligkos, S.; Wernsdorfer, W.; Brechin, E. K.; Papaefstathiou, G. S. *Chem. Commun.* **2011**, 47, 3090.
- (8) CSD Database, ver. 5.33, November 2011.
- (9) Lampropoulos, C.; Stamatatos, T. C.; Abboud, K. A.; Christou, G. *Polyhedron* **2009**, *28*, 1958.
- (10) Brechin, E. K.; Christou, G.; Soler, M.; Helliwell, M.; Teat, S. J. *Dalton Trans.* **2003**, 513.
- (11) Koumoussi, E. S.; Manos, M. J.; Lampropoulos, C.; Tasiopoulos, A. J.; Wernsdorfer, W.; Christou, G.; Stamatatos, T. C. *Inorg. Chem.* **2010**, *49*, 3077.
- (12) Langley, S. K.; Moubaraki, B.; Murray, K. S. *Dalton Trans.* **2010**, 39, 5066.
- (13) Shanmugam, M.; Chastanet, G.; Mallah, T.; Sessoli, R.; Teat, S. J.; Timco, G. A.; Winpenny, R. E. P. *Chem.—Eur. J.* **2006**, *12*, 8777.
- (14) Milway, V. A.; Abedin, S. M. T.; Niel, V.; Kelly, T. L.; Dawe, L. N.; Dey, S. K.; Thompson, D. W.; Miller, D. O.; Alam, M. S.; Muller, P.; Thompson, L. K. *Dalton Trans.* **2006**, 2835.
- (15) Murrie, M.; Parsons, S.; Winpenny, R. E. P. *J. Chem. Soc., Dalton Trans.* **1998**, 1423.
- (16) Low, D. W.; Eichhorn, D. M.; Draganescu, A.; Armstrong, W. H. *Inorg. Chem.* **1991**, *30*, 877.
- (17) Murugesu, M.; Wernsdorfer, W.; Christou, G.; Brechin, E. K. *Polyhedron* **2007**, *26*, 1845.
- (18) Chakov, N. E.; Zakharov, L. N.; Rheingold, A. L.; Abboud, K. A.; Christou, G. *Inorg. Chem.* **2005**, *44*, 4555.
- (19) Wang, M.; Ma, C.; Chen, C. *Dalton Trans.* **2008**, 4612.
- (20) Considering the following Hamiltonian: $H = DS_z^2$.